AGU PUBLICATIONS

Geophysical Research Letters

RESEARCH LETTER
10.1002/2014GL059760

Key Points:
- The effect of emissions on heavy precipitation events may be highly local
- The effect of emissions on extreme temperatures can be spatially generic
- The spatial pattern of extreme precipitation trends may be poorly understood

Supporting Information:
- Readme
- Figures S1 and S2

Correspondence to:
D. A. Stone,
dstone@lbl.gov

Citation:
Angélil, O., D. A. Stone, and P. Pall (2014), Attributing the probability of South African weather extremes to anthropogenic greenhouse gas emissions: Spatial characteristics, *Geophys. Res. Lett.*, *41*, 3238–3243, doi:10.1002/2014GL059760.

Received 28 FEB 2014
Accepted 14 APR 2014
Accepted article online 22 APR 2014
Published online 5 MAY 2014

Attributing the probability of South African weather extremes to anthropogenic greenhouse gas emissions: Spatial characteristics

Oliver Angélil[1], Dáithí A. Stone[1], and Pardeep Pall[2]

[1]Climate Systems Analysis Group, Environmental and Geographical Science, University of Cape Town, Rondebosch, South Africa, [2]Institute for Atmospheric and Climate Science, ETH Zurich, Zurich, Switzerland

Abstract Recent studies have examined the role of anthropogenic emissions in the probability of extreme weather events. These studies examine an event aggregated over a spatial domain, but the dependence on domain definition is unknown. Here we investigate this dependence for the frequency of daily weather extremes across South Africa using a climate model run under both a real-world and a nongreenhouse gas world scenario. Attributable changes in extremely hot and cold days are dominated by large-scale spatial structures, with sharp gradients at the 100 km scale arising for hot events because of the large magnitude of changes. The attributable probabilities of heavy precipitation events are spatially heterogeneous down to the 100 km resolution of the climate model. Therefore, while estimates of attributable probability for temperature events may often be considered valid within smaller and neighboring spatial domains, it appears that estimates for heavy daily precipitation events may be sensitive to the definition of the event.

1. Introduction

Recent years have witnessed a number of unusual and damaging weather events around the world. A frequent question asked by the public and news media was whether the likelihood of such events has been altered as a part of climate change due to anthropogenic emissions [*Stott*, 2010; *Schiermeier*, 2011] and thus whether our past activities are in part responsible for any damage caused [*Grossman*, 2003; *Allen*, 2003; *Allen and Lord*, 2004]. A number of studies have since analyzed this attribution question in detail for various weather events of the past decade [e.g., *Peterson et al.*, 2012, 2013; *Shiogama et al.*, 2013; *Stott et al.*, 2013], while real-time attribution statements of predefined event definitions are now being produced in an operational format (http://www.csag.uct.ac.za/~daithi/forecast).

Such studies form a new field of attribution research, with a number of scientific questions that still need to be explored. One such question is how attribution results vary geographically at regional scales of millions of kilometers squared and smaller. In Africa this question is especially acute, because of the lack of high-density station monitoring that can be leveraged in attribution studies. Also, within any proactive attribution service it will only be possible to examine a limited number of regional definitions of weather events, which inevitably will not fit neatly into the pattern of events that actually ends up occurring. This paper presents a first examination of this issue of spatial scale through an investigation of attribution results for the probability of daily temperature and daily and monthly precipitation extremes over South Africa and neighboring regions. Results are estimated from a time-slice experimental setup which compares large ensembles of relatively high-resolution climate model simulations run under April 2000 to March 2001 conditions, both with and without the influence of anthropogenic greenhouse gas emissions. The relevance of daily temperature and precipitation extremes to the risk of impacts depends on the nature of the hazard considered and changes in nonclimate drivers [*Huggel et al.*, 2013], and so results should be viewed in a general indicative context without specific relevance to any particular extreme weather-related damage that has been experienced thus far.

2. Data and Model

We use data from the experiment of *Pall et al.* [2011] and *Pall* [2007]. Their study assessed the anthropogenic contribution of historical greenhouse gas emissions to the chance of autumn 2000 floods in England and

Wales. Their atmospheric climate model also output daily mean temperature and total precipitation values over a South African domain which we use in this study. The model used was HadAM3-N144—a dynamical atmospheric model with global horizontal resolution of 1.25° longitude and 0.83° latitude [*Pope and Stratton*, 2002]. All HadAM3-N144 simulations had initial conditions set with small random perturbations to a single arbitrary state (unrelated to the actual observed state of 1 April 2000), in order to account for a variety of different plausible realizations of the April 2000 to March 2001 weather under contemporary climate conditions. Due to the nature of these initial conditions, the simulations do not provide a full indication of the range of possible initial weather in April 2000; however, because April is outside of the wet, hot, or cold seasons in southern Africa this should not affect the relevance of our analysis of daily extremes for the full annual period.

In order to realistically simulate the real-world April 2000 to March 2001 climate, HadAM3-N144 simulations were run under a scenario intended to represent year 2000–2001 boundary conditions on the atmosphere, including atmospheric concentrations of radiatively important gases and sulfate aerosols, and weekly varying sea surface temperatures (SSTs) and sea ice concentrations (SICs). A parallel scenario was used to explore a hypothetical climate in which human activities had never emitted twentieth century greenhouse gases, by reducing greenhouse gas concentrations to year 1900 levels, cooling SSTs by an estimate of the twentieth century warming attributable to anthropogenic greenhouse gases emissions, and expanding SICs in accordance with this SST cooling [*Pall et al.*, 2011; *Pall*, 2007]. A number of different samples of this nongreenhouse gas scenario were used to account for uncertainty in the estimate of attributable SST warming. This was done through the use of pattern signals of warming estimated from four coupled ocean-atmosphere models, each with 10 possible amplitudes estimated as the deciles of the probability distributions of the regression coefficient for the greenhouse gas response in the attribution analyses of *Stott et al.* [2006] and *Nozawa et al.* [2005]. To gain sampling power, we have pooled simulations from the first and second deciles, the third and fourth deciles, etc. for this paper, resulting in five amplitude estimates of attributable warming for each of the four pattern signal estimates. Simulations were run using the http://climateprediction.net facility on volunteered home computers around the world, allowing unprecedentedly large ensembles to be generated—each representing the climate associated with a given driving scenario. Full details are given in *Pall et al.* [2011] and *Pall* [2007]. In this study we examine data from 868 simulations from both the real-world climate and each of the 20 hypothetical nongreenhouse gas climate estimates.

3. Methodology

We select precipitation and temperature thresholds for daily extremes from the simulations driven by the real-world scenario. A 1-in-1-year threshold (providing 87,494 days sampled beyond the threshold in the real-world simulations) is used for the temperature events as events of this magnitude appear to be representative of the extreme tails across the country (not shown) and, for hot days, they remain fairly well sampled in the nongreenhouse gas simulations. A higher threshold, 1-in-10-year (8749 days sampled), is used for precipitation events, however, as lower thresholds appear inadequate for representing the extreme tails in some of the more arid zones. The precipitation thresholds exhibit a smooth spatial gradient from lower values along the western coast (~40 mm) to nearly 200 mm in eastern Mpumalanga (the northeast) and neighboring areas of Mozambique. The temperature thresholds follow a more complicated distribution following topography, with lowest values over the Lesotho Highlands and the Central Plateau of Namibia and highest values toward Mozambique and, in the case of hot thresholds, the western coast. Coastal values in the model are likely to be partly constrained by the imposed SSTs offshore and thus not reflective of the real possible magnitude of extremes.

We use the "Risk Ratio" (RR) to measure the change in chance of the event between the two scenarios. If the fraction of days exceeding the threshold under the real-world and the nongreenhouse gas scenarios are represented by P_{real} and P_{nonGHG}, respectively, then the RR is given by $P_{\mathrm{real}}/P_{\mathrm{nonGHG}}$. Given our large sample sizes and not-too-rare thresholds, we do not encounter cases where P_{nonGHG} is empirically zero. While strictly speaking we are not investigating risk, the RR is the common term for measuring this ratio and so we retain it here.

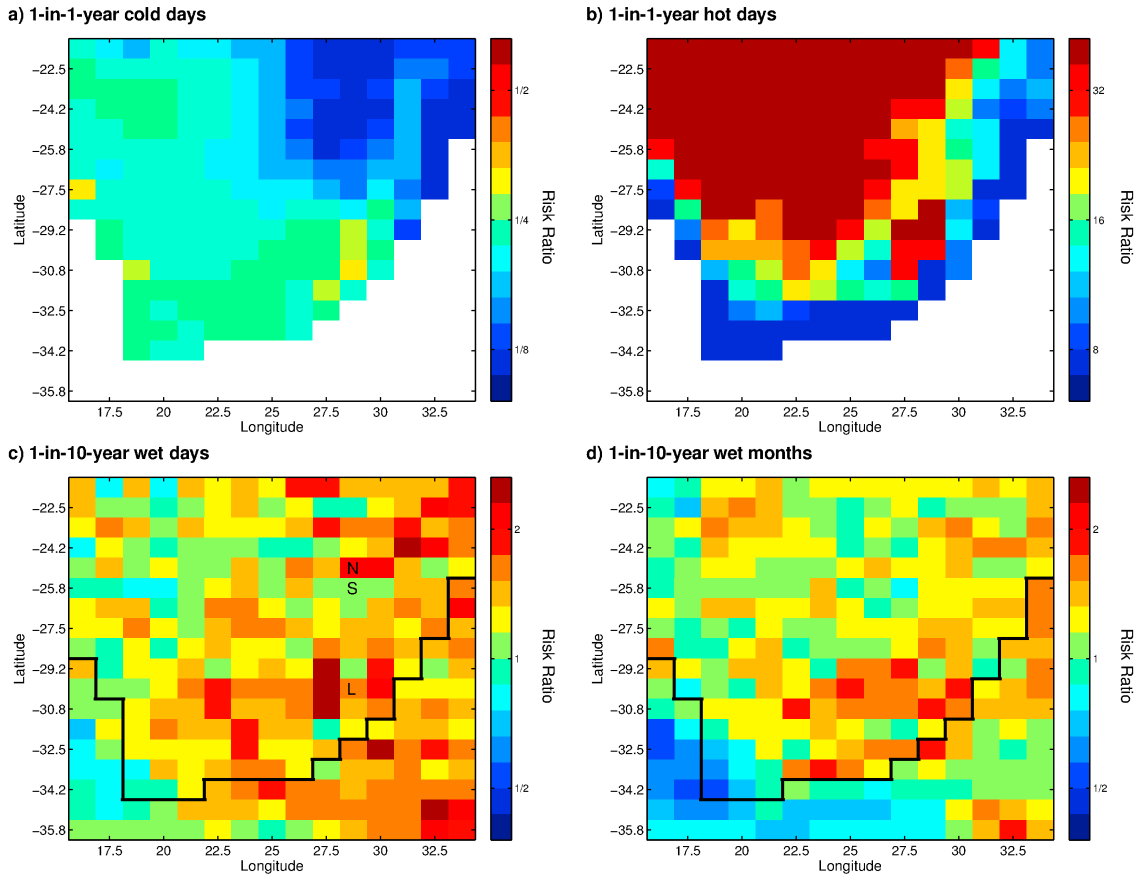

Figure 1. Maps of the best estimate of Risk Ratios due to twentieth century greenhouse gas emissions: (a) 1-in-1-year cold day, (b) 1-in-1-year hot day, (c) 1-in-10-year wet day, and (d) 1-in-10-year wet month. Values are means of the best estimate Risk Ratios obtained with respect to each of the 20 estimates of the nongreenhouse gas scenario. In Figure 1c the “L” marks the approximate center of Lesotho, while the “N” and “S” mark the grid cells across the northern edge of the Highveld plateau in Mpumalanga examined in Figure 2.

4. Results

The best estimate RR values for the extreme temperature and heavy daily precipitation events are calculated as the means of the aggregate distributions of the 20 separate estimates generated using each of the 20 estimates of the nongreenhouse gas climate. The map for unusually cold days (Figure 1a) has lowest values over the Lesotho Highlands (see Figure S1 in the supporting information for a map of orography and political borders) and highest values over Limpopo (the more moist northeast). Spatial gradients are fairly smooth, occur at large scales, and overall the RR spans only about a factor of 2 across the region.

The pattern for unusually hot days differs in some respects (Figure 1b). In this case the difference is mostly lower values in areas of the south and east (with values below an 8 times increase in the chance) and much higher values in the northwestern desert regions. This large-scale result is intuitive, as temperature variability decreases toward the equator. Against this large-scale structure there is also a small area of high values around the Lesotho Highlands (in the southeast of the map), and overall the range of RR values is much larger, in a logarithmic sense, than for cold days. Hence, the gradients can reach a factor of 4 between neighboring grid boxes (a distance of only about 100 km).

The RR map for heavy daily precipitation (Figure 1c) shows further differences from the maps for hot and cold temperature extremes (evident with all three maps spanning the same logarithmic range). In the heavy precipitation map there is a tendency for lower RR values, sometimes less than one, in the west and higher values in the east. This matches the pattern of projected future trends in extreme daily rainfall noted elsewhere [*Kharin et al.*, 2007], but it should be noted that these models lack the landfalling tropical cyclones that are responsible for the most extreme rainfall in the northeast and so this pattern may not be an accurate estimate of the actual Risk Ratio or future trends. However, the main feature of the map is not the

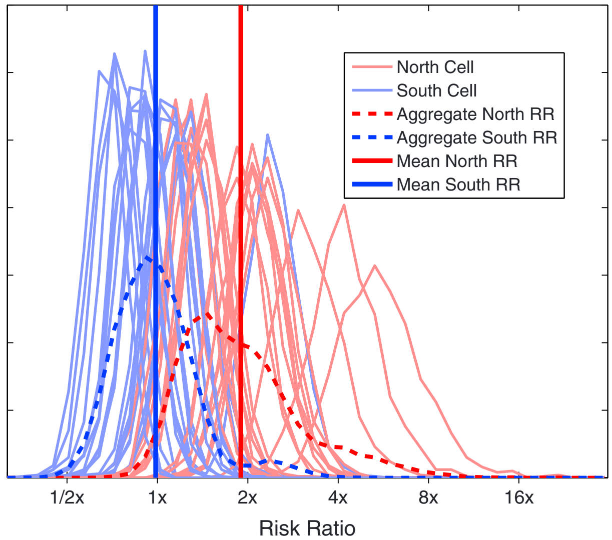

Figure 2. Histograms of the Risk Ratio estimates for heavy daily precipitation for the two grid cells highlighted in Figure 1c. The histograms are generated using a Monte Carlo procedure involving 1000 samples taken from the available collection of real-world and nongreenhouse gas simulations, following *Pall et al.* [2011]. Distributions using each of the 20 nongreenhouse gas scenario estimates are shown separately.

large-scale structure but rather its grid-scale patchiness. In some cases, RR values differ by a factor of 2 between neighboring grid boxes. Some of these sharp differences correspond to locations with steep topographic gradients (for example the three boxes with RR > 2 over western Lesotho), but no consistent pattern is evident. Figure 2 shows details of the RR estimates for two grid boxes across the northern edge of the Highveld plateau in Mpumalanga highlighted in Figure 1c (labeled "N" and "S", see also Figure S1 for the orography). Each of the 20 histograms for either grid box uses one of the 20 nongreenhouse gas climate estimates and was generated from a 1000-member Monte Carlo resampling procedure following *Pall et al.* [2011]. There is some spread in RR estimates for each grid box, dominated by the uncertainty in nongreenhouse gas scenario conditions (the spread in locations of the histograms) rather than sampling uncertainty (the spread of the histograms themselves). Despite this spread, there is a consistent segregation of the histograms for the two grid boxes, with no change in the chance of heavy precipitation due to greenhouse gas emissions in the southern (Highveld) cell but a significant change, and most likely doubling, of the probability in the northern grid box. Notably, histograms on the left-hand side for the southern grid box correspond to histograms on the left-hand side for the northern grid box, and so on, with a robust difference in the RRs of the two cells of about 2 times across all 20 nongreenhouse gas scenario estimates.

Does this spatial heterogeneity extend to other definitions of heavy rainfall events? If a 1-in-1-year threshold is used the map is considerably more smooth (Figure S2), in large part the RR generally ranges only between −15% to +30% across the region. It is unclear how well such a threshold is sampling the processes responsible for generating heavy daily events considering the marked seasonality of precipitation in most of the country; indeed, the return period plots do not yet resemble an exponential tail at this threshold. Thus, such a low threshold may in fact be more representative of changes in mean precipitation than of changes in the wet extreme tail.

Figure 1d shows best estimate RR values for monthly precipitation extremes. A 1-month-in-10-year (0.83% chance for an average month) return period in the real-world climate defines the threshold at each grid cell. While values are generally similar between the two plots, the large-scale spatial structure for 1-day-in-10-year is more visible here. The wet-month map indeed appears to have fewer extreme box-to-box differences than the wet-day map, but it nevertheless contains a number of gradients exceeding 75% between neighboring grid cells.

5. Discussion

The quantitative estimates of attributable changes in the chance of events found in this investigation should be taken with caution. The appropriateness of the HadAM3-N144 atmospheric model in reproducing daily extremes over southern Africa has not been explored in this study. Importantly, the variability generated by the climate model at the grid resolution scale should be lower than the true variability at this scale because the model is not explicitly simulating small-scale processes feeding this variability. Because the RR is to some degree the ratio of the shift in the climatic means between the two scenarios relative to the spread of the variability, the estimates here are thus probably biased away from no change. However, the goal of this paper is to examine the general properties of the spatial variation of attributable probability estimates, and the above issues would affect these qualitative conclusions only if they vary dramatically across South Africa.

The study was restricted to areas in and around South Africa, a subtropical arid region, and it is unclear how far the results can be extrapolated to regions with different climates. Notably, *Kay et al.* [2011] did not note major variations in the attributable probability of very wet days, in data from the same experiment as used here, over England, although that region is covered by a much smaller number of grid boxes and may not be representative of larger continental regions in general.

The RRs for daily cold extremes generally vary as we might intuitively expect, matching the pattern of long-term observed trends [*Kruger and Sekele*, 2013]. In particular, variations occur over scales larger than several hundred kilometers. Thus, estimates of attributable probability for any particular area can generally be considered valid for regions within that area as well as neighboring regions. While the pattern similarly matches observed trends [*Kruger and Sekele*, 2013], the situation with hot days differs in some respects, with the sheer magnitude of the changes in probability resulting in strong gradients even at the grid resolution of the climate model ($\sim$100 km). The discrepancy amounts to the overall magnitude of changes which is in large part a consequence of the convention of thresholds based on the recent "real-world" climate, which has been followed here (albeit in exaggerated form). For hot days, the threshold lies in the approximately exponential tail of the distribution, but for cold days it is much more in the main part of the distribution of the "non-GHG-world" climate and thus the chance of threshold exceedance cannot change as much [*Otto et al.*, 2012].

The situation with extremely wet days differs even more. Variations predominantly occur at the grid resolution of the climate model ($\sim$100 km) rather than at the larger scale, and they are much larger than can be accounted through sampling error. Could this be an artifact of the HadAM3-N144 model? It could be that numerical issues induce odd behavior in the changes of precipitation extremes at the grid resolution, especially in areas of high topographical variation. However, sample tests using averages over 3×3 grid boxes indicate that a similar roughness occurs with that more physically plausible aggregation (not shown). For the moment though, no sufficiently large ensemble has been generated with another climate model for comparison.

Looking beyond climate model output, analyses of trends in indices of extreme precipitation in observational measurements lend further support to a spatially complicated response to external forcings. For instance, in the trend analysis of *Mason et al.* [1999] there are a number of stations at which significantly negative trends and significantly positive trends have occurred within 1000–200 km of each other, even while the general tendency is for positive trends. Fewer such cases are visible in the study of *Kruger* [2006], which effectively uses lower thresholds, but nevertheless there are a number of sites with large statistically significant positive trends which are well within 100 km of sites with small, even negative, statistically insignificant trends; while it is unclear whether there is a significant disagreement between these neighboring stations, it does imply little relationship between trends at neighboring locations. Of course, these studies note that there is some question concerning consistency of the quality of the station measurements, which could give rise to these discrepancies. However, similar spatial heterogeneity can be seen in observational trend studies in some other parts of the world, even if not in others [e.g., *Min et al.*, 2011].

At the very least, for now estimates of attributable changes in probability for heavy precipitation events over an arid southern African domain should be considered highly targeted with restricted validity for subdomains or neighboring areas. To a lesser degree, this caution also applies to changes in the chance of hot events. This property may pose a major challenge for operational attribution services. If such services are run in a proactive mode, following predefined regional domains, their relevance to events that end up actually occurring will be limited. On the other hand, if these services are run in a reactive mode, responding to events that have occurred, they may exaggerate existing selection bias problems [*Chase et al.*, 2006]. It is important to note though that changes in local rainfall may not be the main climatic determinant of attributable risk for many hydrological impacts [*Kay et al.*, 2011; *Wolski et al.*, 2014]; in fact the dominant driver of risk may not be climatic at all [*Huggel et al.*, 2013]. Thus, for an informative, unbiased service addressing weather-related impact risk it will be vital to focus on the impact events themselves and to consider the relative importance of all drivers of change.

Acknowledgments
O.A. and D.A.S. were funded by Microsoft Research, with D.A.S. receiving additional support from the U.S. Department of Energy's Office of Science, Office of Biological and Environmental Research, and the U.S. National Oceanic Administration's Climate Program Office, via the International Detection and Attribution Group. P.P. was funded by NCCR Climate. Additional funding from the South African Water Research Commission assisted in completion of the manuscript. The authors wish to thank the http://climateprediction.net group and the individuals around the world who volunteered their computers to run the climate model simulations. The data used in this analysis are available at http://www.climateprediction.net.

The Editor thanks two anonymous reviewers for their assistance in evaluating this paper.

References

Allen, M. (2003), Liability for climate change, *Nature*, *421*, 891–892.

Allen, M. R., and R. Lord (2004), The blame game, *Nature*, *432*, 551–552.

Chase, T. N., K. Wolter, R. A. S. Pielke, and I. Rasool (2006), Was the 2003 European summer heat wave unusual in a global context?, *Geophys. Res. Lett.*, *33*, L23709, doi:10.1029/2006GL027470.

Grossman, D. A. (2003), Warming up to a not-so-radical idea: Tort-based climate change litigation, *Colum. J. Envtl. L.*, *28*, 1–61.

Huggel, C., D. Stone, M. Auffhammer, and G. Hansen (2013), Loss and damage attribution, *Nat. Clim. Change*, *3*, 694–696.

Kay, A. L., S. M. Crooks, P. Pall, and D. A. Stone (2011), Attribution of Autumn/Winter 2000 flood risk in England to anthropogenic climate change: A catchment-based study, *J. Hydrol.*, *406*, 97–112, doi:10.1016/j.jhydrol.2011.06.006.

Kharin, V. V., F. W. Zwiers, X. Zhang, and G. C. Hegerl (2007), Changes in temperature and precipitation extremes in the IPCC ensemble of global couple model simulations, *J. Clim.*, *20*, 1419–1444.

Kruger, A. C. (2006), Observed trends in daily precipitation indices in South Africa: 1910–2004, *Int. J. Climatol.*, *26*, 2275–2285.

Kruger, A. C., and S. S. Sekele (2013), Trends in extreme temperature indices in South Africa: 1962–2009, *Int. J. Climatol.*, *33*, 661–676.

Mason, S. J., P. R. Waylen, G. M. Mimmack, B. Rajaratnam, and J. M. Harrison (1999), Changes in extreme rainfall events in South Africa, *Clim. Change*, *41*, 249–257.

Min, S.-K., X. Zhang, F. W. Zwiers, and G. C. Hegerl (2011), Human contribution to more-intense precipitation extremes, *Nature*, *470*, 378–381.

Nozawa, T., T. Nagashima, H. Shiogama, and S. A. Crooks (2005), Detecting natural influence on surface air temperature change in the early twentieth century, *Geophys. Res. Lett.*, *32*, L20719, doi:10.1029/2005GL023540.

Otto, F. E. L., N. Massey, G. J. van Oldenborgh, R. Jones, and M. R. Allen (2012), Reconciling two approaches to attribution of the 2010 Russian heat wave, *Geophys. Res. Lett.*, *39*, L04702, doi:10.1029/2011GL050422.

Pall, P. (2007), Constraints on, and attribution of, changes in extreme precipitation under climate change, PhD thesis, St. Cross College, Univ. of Oxford, Oxford, U. K.

Pall, P., T. Aina, D. A. Stone, P. A. Stott, T. Nozawa, A. G. J. Hilberts, D. Lohmann, and M. R. Allen (2011), Anthropogenic greenhouse gas contribution to flood risk in England and Wales in Autumn 2000, *Nature*, *470*, 382–385.

Peterson, T. C., et al. (2012), Explaining extreme events of 2011 from a climate perspective, *Bull. Am. Meteorol. Soc.*, *93*, 1041–1067.

Peterson, T. C., et al. (2013), Explaining extreme events of 2012 from a climate perspective, *Bull. Am. Meteorol. Soc.*, *94*, S1–S74.

Pope, V. D., and R. A. Stratton (2002), The processes governing horizontal resolutation sensitivity in a climate model, *Clim. Dyn.*, *12*, 211–236.

Schiermeier, Q. (2011), Extreme measures, *Nature*, *477*, 148–149.

Shiogama, H., M. Watanabe, Y. Imada, M. Mori, M. Ishii, and M. Kimoto (2013), An event attribution of the 2010 drought in the South Amazon region using the MIROC5 model, *Atmos. Sci. Lett.*, *14*, 170–175.

Stott, P. (2010), Climate change: How to play our hand?, Guardian.

Stott, P. A., J. F. B. Mitchell, M. R. Allen, T. L. Delworth, J. M. Gregory, G. A. Meehl, and B. D. Santer (2006), Observational constrains on past attributable warming and predictions of future global warming, *J. Clim.*, *19*, 3055–3069.

Stott, P. A., M. R. Allen, N. Christidis, R. Dole, M. Hoerling, C. Huntingford, P. Pall, J. Perlwitz, and D. A. Stone (2013), Attribution of weather and climate-related extreme events, in *Climate Science for Serving Society: Research, Modelling and Prediction Priorities*, edited by G. R. Asrar and J. W. Hurrell, pp. 307–337, Springer, Dordrecht, Netherlands.

Wolski, P., D. Stone, M. Tadross, M. Wehner, and B. Hewitson (2014), Attribution of floods in the Okavango Basin, Southern Africa, *J. Hydrol.*, *511*, 350–358.

